Oct 18th, 12:00 AM

Buckling Behaviour of Cold-formed Thin-walled Members by Spline Finite Strip Analysis

Joachim Lindner

Y. L. Guo

Twelfth International Specialty Conference on Cold-Formed Steel Structures
St. Louis, Missouri, U.S.A., October 18-19, 1994

Buckling Behaviour of Cold-Formed Thin-Walled Members by Spline Finite Strip Analysis

J.Lindner* & Y.L.Guo**

Abstract: *Local, distortional and overall buckling (including overall flexural buckling and overall flexural-torsional buckling) behaviour of cold-formed thin-walled columns is presented which is based on an inelastic spline finite strip analysis. The columns are loaded centrally at the ends. The increment of yield stresses in the corner area due to cold-forming work, together with a more real stress-strain curve of material, that exhibits continuous strain hardening for the stress above the proportional limit of material, are involved in the analysis. The cold-formed section is divided into two different types of strips, one is a flat plate strip on the central part of the plates while the other is a cylinderical shell strip at the corner area. The circular corner effect, which is formed during the manufacture process, is taken into account in the computer programme. A lot of numerial results are obtained, which reveal that the inelastic distortional buckling behaviour is very important.*

1. Introduction

According to the traditional buckling theory, the buckling modes of thin-walled members are divided into two different types: local buckling and overall buckling (including flexural buckling, torsional buckling, and flexural-torsional buckling). The interaction buckling, however, often takes place in thin-walled members.

In general, the interaction buckling of thin-walled members are classified into two different types according to whether the post local buckling strength of plates is taken into account. They are called as bifurcation interaction buckling and ultimate interaction buckling, respectively. The first is the interaction buckling where two or more buckling modes interact and take place in the form of coupling buckling simultaneously or nearly simultaneously. Often this interaction is known as distortional buckling. It is evident that the buckling load of the

* Prof. Dr., Institut fuer Baukonstruktionen und Festigkeit, TU Berlin, Germany;
**Associate Prof. Dr., Department of Civil Engineering, Northwestern Polytechnical University, Xian, China;

The second author is supported by the fellowship from the Alexander von Humboldt Foundation of Germany

distortional buckling is less than the buckling loads of all independent buckling modes which participate in the interaction between or among them. The second is the interaction buckling where the plate elements do go into post local buckling range. This situation often takes place for thin-walled members which have larger width-thickness ratios of plates and a medium slender ratio of the member. In other words, this situation occurs only when the local buckling load of the member is less than the overall buckling load of the member. This paper deals with the bifurcation interaction buckling, or distortional buckling in cold-formed thin-walled columns.

In this study the local buckling, distortional buckling and overall buckling behaviour (including flexural buckling and flexural-torsional buckling) of cold-formed thin-walled columns is presented in the inelastic range. A typical stress-strain curve of material for cold-formed section, which exhibits a continuous strain hardening for the stress above the proportional limit of material, is adopted and a flow theory of plasticity is employed in the analysis. In addition the variation of yield stress over the cross section and the circular corner effect due to cold-forming work during the manufature process are taken into account in the coputer programme. To this purpose a kind of cylinderical shell strip is developed to model the circular corner effect on the corner area.

The theoretical analysis is based on the spline finite strip method which has been developed by Fan & Cheung [1] for the stress analysis of shell structure and by Lau & Hancock [2] for the buckling analysis of plated structures. The most advantage of the spline finite strip method that it can automatically predict the lowest buckling load corresponding to some interaction buckling mode and some independent buckling modes, generally from local buckling through distortional buckling into overall buckling with increasing lengths of member. If the finite strip method is used, the number of buckling waveshape has to be continuously adjusted until the lowest buckling load is reached. In addition, the spline finite strip method can apply to any internal and external boundary conditions (including different boundary conditions at the end sections of column) and arbitrary loading types, while the finite strip method only applies to simply supported boundary condition. Meanwhile the spline finite strip method can greatly save computer storage and computational effect compared with the finite element method.

2. Theoretical Analysis

2.1 Material Properties of Cold-Formed Section

Due to the cold-forming effect during the manufacture process, the yield stresses at the corner area are considerably higher than at the central part of the section. It has been shown by Key & Hancock [3] and Lindner &Aschinger [4] that, at the highly hardening corner area, the measured yield stresses are significantly greater than those on the flat part of each plate, and almost show a sudden variation at the transition from the corners to the flat plates. Therefore, a block distribution of the yield stresses is assumed in the analysis, as shown in Fig.1a. The yield stress at the corner area depends on the yield stress and the ultimate strength of the virgin material, as well as the bending radius at the corner. An empirical formula developed by Karren [5] is given in equation (1).

$$\frac{f_{yc}}{f_y} = \frac{B_c}{(r/t)^m} \tag{1}$$

where

$$B_c = 3.69\frac{f_b}{f_y} - 0.819\left(\frac{f_b}{f_y}\right)^2 - 1.79$$

$$m = 0.192\frac{f_b}{f_y} - 0.068$$

In the above expressions, f_{yc} =yield stress at the corner area; f_b =ultimate strength of the virgin material; f_y =yield stress of the virgin material; r =bending radius at the corners; t =thickness of flat plate.

In general, the stress-strain curve of cold-formed material, as shown in Fig.1b, exhibits continuous strain hardening for the stress above the proportional limit of material to fully yielding. Chajies and Fang [6] have proposed that it is reasonable to introduce the tangential modulus expression for the hot-rolled members developed by Bleich [7] into the cold-formed members. From this expression a dimensionless stress-strain curve, as shown in Fig.1b, is derived as follows [8]:

$$\bar{\sigma} = \begin{cases} \bar{\epsilon} & \bar{\epsilon} \le \bar{\epsilon_p} \\ \frac{\psi e^{c(\bar{\epsilon}-\bar{\epsilon_p})}}{1+\psi e^{c(\bar{\epsilon}-\bar{\epsilon_p})}} & \bar{\epsilon} > \bar{\epsilon_p} \end{cases} \tag{2}$$

in which

$$\bar{\sigma} = \frac{\sigma}{f_y} \quad \bar{\sigma_p} = \frac{f_p}{f_y} \quad \bar{\epsilon} = \frac{\epsilon}{\epsilon_y} \quad \bar{\epsilon_p} = \frac{\epsilon_p}{\epsilon_y}$$

$$c = [\frac{f_p}{f_y}(1 - \frac{f_p}{f_y})]^{-1} \quad \psi = \frac{\bar{\epsilon_p}}{(1 - \bar{\epsilon_p})} = \frac{\bar{\sigma_p}}{(1 - \bar{\sigma_p})}$$

It is assumed that the yield stress at the corner area has the same form as shown in Fig.1b. However, all parameters used in equation (2) should be replaced by those corresponding to the materials at the corners, and that the proportional limit of material at the corners takes the same times as the f_{yc} relative to f_y, or $f_{pc} = f_p f_{yc}/f_y$.

2.2 Spline Finite Strip Formulation

2.2.1 Spline Finite Strip Displacement Function

The general theory and application of the spline finite strip method have been described by Fan & Cheung [1] for the stress analysis of shallow shells and by Lau & Hancock [2] for the buckling analysis of plated structures. However, in this study, a combination of flat plate strips and cylinderical shell strips, as shown in Fig.2a and 2b, is used to model the cold-formed section columns, as shown in Fig.1a.

A typic spline finite strip with four equal sections is expressed as fellows:

$$\Phi_i = \frac{1}{6h^3} \begin{cases} 0, & x \le x_{i-2} \\ (x - x_{i-2})^3, & x_{i-2} \le x \le x_{i-1} \\ h^3 + 3h^2(x - x_{i-1}) + 3h(x - x_{i-1})^2 - 3(x - x_{i-1})^3, & x_{i-1} \le x \le x_i \\ h^3 + 3h^2(x_{i+1} - x) + 3h(x_{i+1} - x)^2 - 3(x_{i+1} - x)^3, & x_i \le x \le x_{i+1} \\ (x_{i+2} - x)^3, & x_{i+1} \le x \le x_{i+2} \\ 0, & x_{i+2} \le x \end{cases}$$

The spline displacement functions for u,v and w along longitudinal direction of the member are thus expressed as a linear combination of $(m+3)$ local B_3 spline

Amended Boundary Local B_3-spline Functions

Boundary Conditions	$\bar{\Phi}_{-1}$	$\bar{\Phi}_0$	$\bar{\Phi}_1$
$f(x_0) \neq 0, f'(x_0) \neq 0$	Φ_{-1}	$\Phi_0 - 4\Phi_{-1}$	$\Phi_1 - 0.5\Phi_0 + \Phi_{-1}$
$f(x_0) = 0, f'(x_0) \neq 0$	Eliminated	$\Phi_0 - 4\Phi_{-1}$	$\Phi_1 - 0.5\Phi_0 + \Phi_{-1}$
$f(x_0) = 0, f'(x_0) = 0$	Eliminated	Eliminated	$\Phi_1 - 0.5\Phi_0 + \Phi_{-1}$
$f(x_0) \neq 0, f'(x_0) = 0$	Eliminated	Φ_0	$\Phi_1 - 0.5\Phi_0 + \Phi_{-1}$

functions, and are given by

$$f = \sum_{i=-1}^{m+1} \alpha_i \Phi_i \tag{3}$$

where m is the number of sections along the length of the member, and $\alpha_i (i = -1, 0, 1, ..., m, m+1)$ are coefficients depending on the interpolation function across the transverse direction of a strip.

It is assumed that for the in-plane displacements u, v in the y direction a linear polynomial interpolation is chosen while for the out-plane flexural displacement w, a cubic polynomial interpolation is taken to ensure the deflection and rotation continuities. Due to the location property of the spline function, it is easy to satisfy any prescribed boundary conditions, even different boundary conditions at the same end section by only changing three local spline functions at each end of the column. The amended local boundary spline functions are listed in the Table. Based on the above consideration, the displacement components (u, v, and w) are defined as:

$$\{f\} = [N][\Phi]\{\delta\} \tag{4}$$

where

$$\{f\} = [u, v, w]^T$$

$$[N] = \begin{bmatrix} N_1 & 0 & 0 & 0 & N_2 & 0 & 0 & 0 \\ 0 & N_1 & 0 & 0 & 0 & N_2 & 0 & 0 \\ 0 & 0 & N_3 & N_4 & 0 & 0 & N_5 & N_6 \end{bmatrix}$$

$$[\Phi] = [[\Phi_1] \quad [\Phi_2] \quad [\Phi_3] \cdots [\Phi_6] \quad [\Phi_7] \quad [\Phi_8]]$$

$$\{\delta\} = [\{u_i\}, \{v_i\}, \{w_i\}, \{\theta_i\}, \{u_j\}, \{v_j\}, \{w_j\}, \{\theta_j\}]^T$$

$$[\Phi_i] = [\bar{\Phi}_{-1}, \bar{\Phi}_0, \bar{\Phi}_1, \Phi_2, \cdots, \Phi_{m-2}, \bar{\Phi}_{m-1}, \bar{\Phi}_m, \bar{\Phi}_{m+1}]_i$$

$$N_1 = 1 - (\frac{y}{b}) \quad N_2 = \frac{y}{b}$$

$$N_3 = 1 - 3(\frac{y}{b})^2 + 2(\frac{y}{b})^3 \quad N_4 = y[1 - 2(\frac{y}{b}) + (\frac{y}{b})^2]$$

$$N_5 = [3(\frac{y}{b})^2 - 2(\frac{y}{b})^3] \quad N_6 = y[(\frac{y}{b})^2 - (\frac{y}{b})]$$

2.2.2 Inelastic Stresses-Strains Relation

The general stress-strain relationship for the in-plane and out-plane deformations is written by the following form:

$$\{\sigma\} = [D]\{\epsilon\} \tag{5}$$

in which

$$\{\sigma\} = [\sigma_x, \sigma_y, \sigma_{xy}, M_x, M_y, M_{xy}]^T$$

$$\{\epsilon\} = [\epsilon_x, \epsilon_y, \epsilon_{xy}, \Phi_x, \Phi_y, \Phi_{xy}]^T$$

$$[D] = \begin{bmatrix} [D_M] & 0 \\ 0 & \frac{t^3}{12}[D_M] \end{bmatrix}$$

$$[D_M] = \begin{bmatrix} c_{11} & c_{12} & 0 \\ c_{21} & c_{22} & 0 \\ 0 & 0 & c_{33} \end{bmatrix}$$

$$c_{11} = \frac{E_1}{1 - \nu_1\nu_2}$$

$$c_{12} = c_{21} = \nu_1 c_{22} = \nu_2 c_{11} = \frac{\nu_2 E_1}{1 - \nu_1\nu_2}$$

$$c_{22} = \frac{E_2}{1 - \nu_1 \nu_2}$$

$$c_{33} = G_t$$

In the elastic range, $E_1 = E, \nu_1 = \nu_2 = \nu, G_t = E/2(1 + \nu)$. In the inelastic range the material property coefficients as formulated by Handelman and Prager [9] according to the flow theory of plasticity are given by:

$$E_1 = E_t$$

$$E_2 = \frac{4}{3k + 1} E_t$$

$$\nu_1 = \frac{(2\nu - 1)k + 1}{2}$$

$$\nu_2 = \frac{2[(2\nu - 1)k + 1]}{3k + 1}$$

$$G_t = \frac{1}{2(1 + \nu)k} E_t$$

$$k = \frac{E_t}{E}$$

and the material property coefficients as conducted by Bijlaard [10] according to the deformation theory of plasticity in the inelastic range are given by:

$$E_1 = E_t$$

$$E_2 = \frac{4}{3k(1 + e) + 1} E_t$$

$$\nu_1 = \frac{(2\nu - 1)k + 1}{2}$$

$$\nu_2 = \frac{2[(2\nu - 1)k + 1]}{3k(1 + e) + 1}$$

$$G_t = \frac{1}{[2(1+\nu)+3e]k} E_t$$

$$e = \frac{E}{E_s} - 1$$

where E is the modulus of elasticity, E_t the tangent modulus of material, E_s the secant modulus of material, which are determined from the stress-strain curve of material, and ν Poisson's ratio of elasticity.

For the trilinear stress-strain model (perfect elastic plastic material with linear strain hardening), the material properties are based on the results derived by Handelman and Prager [9] with the tangent shear modulus, G_t, being modified according to Lay [11] in order to be applicable for the tirlinear stress-strain curve of material. It is assumed that for the tangent modulus in the yield plateau the same value is taken as the hardening range with a hardening modulus E_{st} instead of zero. These material properties, which are based on a derivation from the flow theory of plasticity, have been used by Dawe and Kulak [12] for local buckling analysis of hot-rolled sections and by Bradford [13] for inelastic local buckling analysis of fabricated I-beams with uniform bending. The amened tangent shear modulus is given as fellows:

$$G_t = \frac{4}{4k(1+\nu)+1} E_t$$

2.2.3 Stiffness Matrix and Geometric Stiffness Matrix

For a cylinderical shell strip the relationship between strains and displacements in the geometric linear theory of shell are expressed by

$$\epsilon_x = \frac{\partial u}{\partial x} \quad \epsilon_y = \frac{\partial v}{\partial y} + \frac{w}{r} \quad \epsilon_{xy} = \frac{\partial u}{\partial y} + \frac{\partial v}{\partial x} \tag{6}$$

$$\Phi_x = -\frac{\partial^2 w}{\partial^2 x} \quad \Phi_y = -\frac{\partial^2 w}{\partial^2 y} \quad \Phi_{xy} = -2\frac{\partial^2 w}{\partial x \partial y} \tag{7}$$

Substituting equation (4) into (6) and (7) gives a relationship relating $\{\epsilon\}$ to $\{\delta\}$ as fellows:

$$\{\epsilon\} = [B]\{\delta\} \tag{8}$$

where

$$[B] =$$

$$\begin{bmatrix}
N_1[\Phi_1'] & 0 & 0 & 0 & N_2[\Phi_3'] & 0 & 0 & 0 \\
0 & N_1'[\Phi_2] & \frac{1}{r}N_3[\Phi_5] & \frac{1}{r}N_4[\Phi_6] & 0 & N_2'[\Phi_4] & \frac{1}{r}N_5[\Phi_7] & \frac{1}{r}N_6[\Phi_8] \\
N_1'[\Phi_1] & N_1[\Phi_2'] & 0 & 0 & N_2'[\Phi_3] & N_2[\Phi_4'] & 0 & 0 \\
0 & 0 & -N_3[\Phi_5"] & -N_4[\Phi_6"] & 0 & 0 & -N_5[\Phi_7"] & -N_6[\Phi_8"] \\
0 & \frac{1}{r}N_1'[\Phi_5] & -N_3"[\Phi_5] & -N_4"[\Phi_6] & 0 & \frac{1}{r}N_2'[\Phi_4] & -N_5"[\Phi_7] & -N_6"[\Phi_8] \\
0 & \frac{2}{r}N_1[\Phi_2'] & -2N_3'[\Phi_5'] & -2N_4'[\Phi_6'] & 0 & \frac{2}{r}N_2[\Phi_4'] & -2N_5'[\Phi_7'] & -2N_6'[\Phi_8']
\end{bmatrix}$$

Using the variation principle with respect to the strain energy given by

$$U = \frac{1}{2}\int_A \{\epsilon\}^T\{\sigma\}dA \tag{9}$$

one can get the stiffness matrix

$$[K] = \int_A [B]^T[D][B]dA$$

If only considering the axial stress and shear stress acting on the four edges of a strip, the increment of potential energy of membrance stresses (σ_x and σ_{xy}) resulting from both flexural buckling deformations and in-plan buckling deformations are given by:

$$W_{\sigma_x+\sigma_{xy}} = -\frac{1}{2}\int_A \{\sigma_x[(\frac{\partial w}{\partial x})^2 + (\frac{\partial u}{\partial x})^2 + (\frac{\partial v}{\partial x})^2] + 2\sigma_{xy}(\frac{\partial w}{\partial x})(\frac{\partial w}{\partial y})\}tdxdy \tag{10}$$

For the flat plate strip, the strain energy resulting from the stress σ_y, which is given by equation (11), is also added to the equation (10).

$$W_{\sigma_y} = -\frac{1}{2}\int_A \{\sigma_y[(\frac{\partial w}{\partial y})^2 + (\frac{\partial u}{\partial y})^2 + (\frac{\partial v}{\partial y})^2]\}tdxdy \tag{11}$$

By using the variation principle with respect to $\{\delta\}$

$$\frac{\partial(W_{\sigma_x+\sigma_{xy}} + W_{\sigma_y})}{\partial\{\delta\}} = 0 \tag{12}$$

one can obtain the geometric stiffness matrix:

$$[G] = [G]_{\sigma_x} + [G]_{\sigma_y} + [G]_{\sigma_{xy}} \tag{13}$$

where

$$[G]_{\sigma_x} = -\int_A ([N][\Phi'])^T N_x [N][\Phi'] dxdy$$

$$[G]_{\sigma_y} = -\int_A ([N'][\Phi])^T N_y [N'][\Phi] dxdy$$

$$[G]_{\sigma_{xy}} = -2\int_A ([N][\Phi'])^T N_{xy} [N'][\Phi] dxdy$$

2.2.4 Matrix Transformation

Before forming the global stiffness matrix and geometric stiffness, the stifness matrix and geometric stiffness of a strip in the local coordinate system should be transformed into the global coordinate system. This transformation is described in Fig.2c. If $\{\Delta\}$ represents nodal displacements of the strips in the global coordinate system the transformed relationship is given by

$$\{\delta\} = [R]\{\Delta\} \tag{14}$$

where

$$[R] = \begin{bmatrix} [R_1] & 0 \\ 0 & [R_2] \end{bmatrix}$$

$$[R_1] = \begin{bmatrix} [I] & 0 & 0 & 0 \\ 0 & [C_1] & [S_1] & 0 \\ 0 & -[S_1] & [C_1] & 0 \\ 0 & 0 & 0 & [I] \end{bmatrix}$$

$$[R_2] = \begin{bmatrix} [I] & 0 & 0 & 0 \\ 0 & [C_2] & [S_2] & 0 \\ 0 & -[S_2] & [C_2] & 0 \\ 0 & 0 & 0 & [I] \end{bmatrix}$$

In the above expressions the $[I]$ is unit matrix, and $[C_i], [S_i](i = 1, 2)$ are diagonal matrices, in which the diagonal elements are equal to $C_i = cos\beta_i, S_i = sin\beta_i (i = 1, 2)$, respectively. For a flat plate strip it is evident that $[C_1] = [C_2] = [C], [S_1] = [S_2] = [S]$.

2.2.5 Solution of the Eigenvalue Problem

After the global stiffness matrix and geometric stiffness matrix are formed, the eigenvalue problem, which is concerned with the determination of local, distortional and overall buckling loads and corresponding modes, is presented by

$$\{[K] - \lambda[G]\}\{\Delta\} = \{0\} \tag{15}$$

In the inelastic range the critical state correspondes to $\lambda = 1$. In this study an iteration procedure is used to determine the lowest eigenvalue and corresponding eigenvectors. To this purpose the above equation is then transformed into the following form:

$$\{[K]^{-1}[G] - \frac{1}{\lambda}[I]\}\{\Delta\} = \{0\} \tag{16}$$

The iteration gives the highest value of $1/\lambda$, or the lowest λ.

3. Numerical Results

As the first example, the effect of the circular corner on the buckling behaviour is investigated theoretically, and shown in Fig.3. The angle section column under uniform compression is selected where the column is simply supported at the ends. It is evident from the figure that the buckling stress of the column increases with the bending radius of the corner.

As the second example as shown in the Fig.4, two different strips, namely cylinderical shell strips and flat plate strips, are used, respectively, to analyse a shallow shell subjected to uniform compression in the longitudinal direction of the shell. The shallow shell is considered as an assembly of a number of flat plate strips when using flat plate strip. The boundary conditions at the four edges of the

shell are described as fellows: u =free,$v = w = 0, \partial w/\partial y = 0$. When the radius of the shell is increased the difference between both results calculated by using the flat plate strip and cylinderical shell strips, respectively, becomes smaller and smaller. When the radius of the shell approaches infinity the buckling stress is equal to the buckling stress of the flat plate ,denoted by σ_0.

Fig.5 shows a relationship between the buckling stress and the length of the column with a hat section and under uniform compression. Three thicknesses of the plate are selected, namely $t = 0.1cm, 0.2cm$ and $0.3cm$. The boundary conditions take u =free,$v = w = 0, \partial v/\partial x \neq 0, \partial w/\partial x \neq 0, \partial v/\partial y \neq 0, \partial w/\partial y \neq 0$, at $x = 0, L$, respectively. The geometric dimensions are $b_w = 10cm, b_f/b_w = 0.25, b_l/b_f = 0.5$. The material properties are $f_y = 24kN/cm^2, f_p = 16kN/cm^2, E = 2.1 \times 10^4 kN/cm^2$, and $\nu = 0.3$. The computational results corresponding to the thickness of the plate $t = 0.1cm$ almost fully fall within the elastic range. The four different buckling modes, namely unsymmetric local buckling mode, symmetric local buckling mode, distortional buckling mode, and flexural- torsional buckling mode, are described in the Fig.6, which correspond to different lengths of the columns, namely $L = 5cm, 10cm, 75cm$ and $120cm$. It was found that the interaction action is more serious when the local buckling load and the overall flexural-torsional buckling load are almost identical. The computed results for the plates with the thicknesses of $0.2cm$ and $0.3cm$ reveal the distorsional buckling involvs in the inelastic range. Therefore the inelastic distortional buckling behaviour is very important for the column with intermedium slender ratio and with intermedium width thickness ratios of the plates forming the column. Fig.7 also gives the computed results of the column with the same shape as Fig.6 but with different dimensions. It is seen that the distorsional buckling of the columns with plate thicknesses of $t = 0.15cm$ and $2.5cm$, both falls within the inelastic range.

4. Conclusions

A spline finite strip computer pragramme has been presented for analysing the local buckling, distorsional buckling and overall buckling of cold-formed thin-walled columns in the elastic and inelastic range, respectively. The corner effect has been taken into account in the analysis. The computed results has revealed that inelastic distorsional buckling behaviour is very important for the

column with intermedium slender ratio and with intermedial width thickness ratios of the plates forming the column. The further theoretical investigation to the cold-formed thin-walled columns with eccentric loading and the cold-formed thin-walled beams with combined loadings of axial compression, transversely concentrated loads, and unequal end moments, is under the way.

References

[1] S.C. Fan & Y.K. Cheung, Analysis of shallow shells by spline finite strip method, *Engineering Structures*, Vol.5, 1983, pp.255-262.

[2] S.C.W. Lau & G.J. Hancock, Inelastic buckling analysis of beams, columns and plates using the spline finite strip method, *Thin-Walled Structures*, Vol.7, 1989, pp.213-238.

[3] P.W. Key & G.J. Hancock, An experimental investigation of the column behaviour of cold-formed square hollow sections, No.R.493, School of civil and mining engineering, University of Syndey, Australia, June, 1985

[4] J. Lindner & R. Aschinger, Zur Streckgrenzenerhoehung infolge Kaltumformung bei duennwandigen profilen, *Stahlbau*, 62(1993), Heft 6, pp.170-178

[5] K.W. Karren, Corner Properties of cold-formed steel shapes, *J. of Structural Division, ASCE Proceeding*, Vol.93, No.ST1, 1967, pp.401-432

[6] A. Chajes & P.J. Fang, Torsional flexural buckling, elastic and inelastic, of cold-formed thin-walled columns, Cornell University, Research Bulletin 66-1, Ithaca, New York.

[7] F. Bleich, *Buckling Strength of Metal Structures*, McGraw-Hill, New York, 1952.

[8] Y.L. Guo, Local and Overall Interactive Instability of Thin-Walled Box-Section Columns, *J. of Constructional Steel Research*, Vol.22, 1992, 1-19

[9] G.H. Handelman & W. Prager, Plastic buckling of a rectangular plate, Technical Note, NACA, No.1530, 1948.

REFERENCES

[10] P.P. Bijlaard, Theory and tests on the plastic stability of plates and shells, *J. of the Aeronautical Science*, Vol.16, 1949, pp.529-541.

[11] M.G. Lay, Flange local buckling in wide-flange shapes, *J. of the Structural Division, ASCE*, Vol.91, No.ST6,1965.

[12] J.L. Dawe & G.L. Kulak, Plate instability of W shapes, *J. of Structural Enginering, ASCE*, Vol.110, No.6, 1984, pp.1278-1291.

[13] M.A. Bradford, Inelastic local buckling of fabricated I-beams, *J. of Constructional Steel Research*, Vol.7, No.5, 1987, pp.317-334

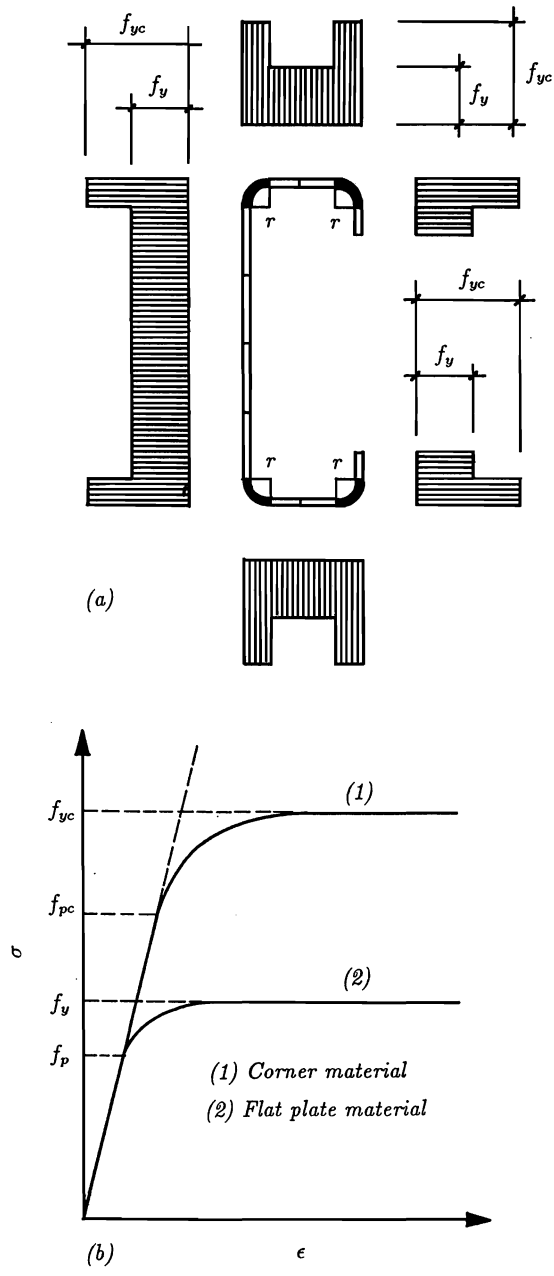

Figure 1: (a) Assumed yield stress distribution; (b) Stress-strain curves of cold-formed materials

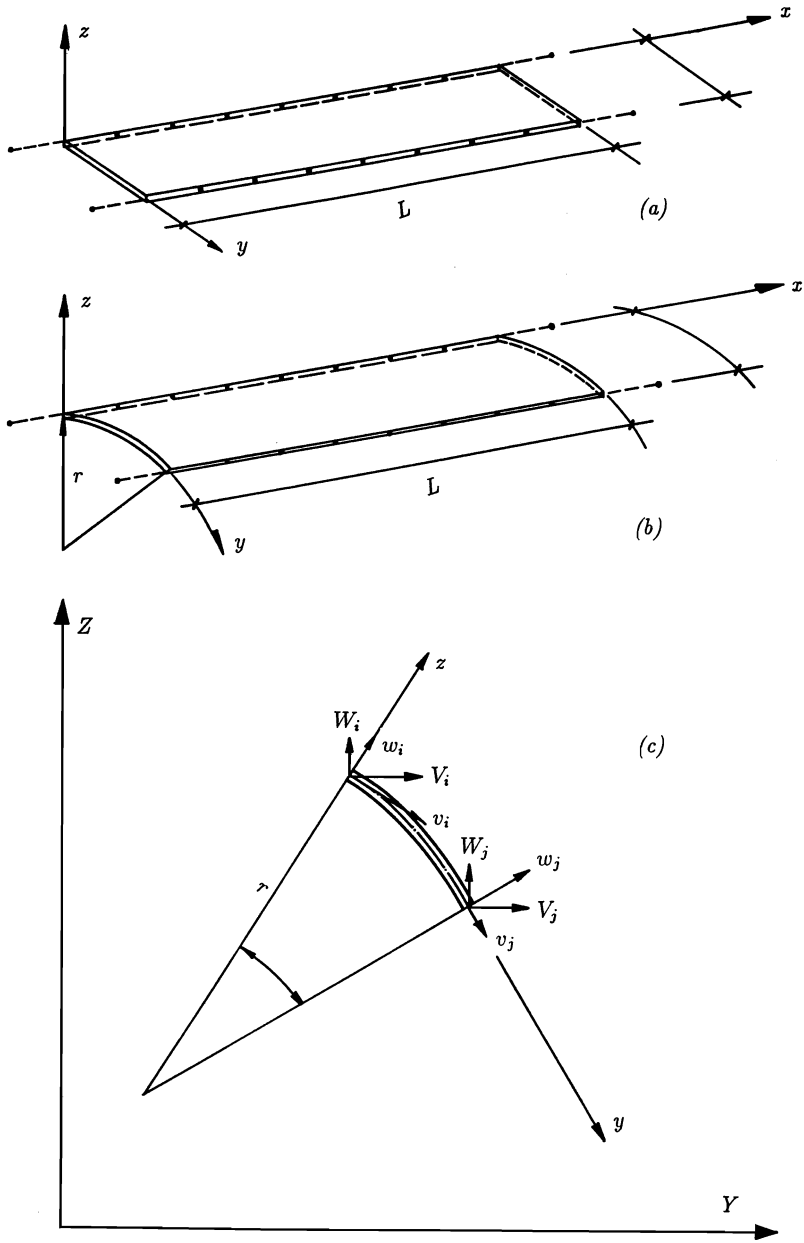

Figure 2: Coordinate system of strips. (a) Flat plate strip; (b) Cylinderical shell strip; (c) Local displacement transformation of cylinderical shell strip

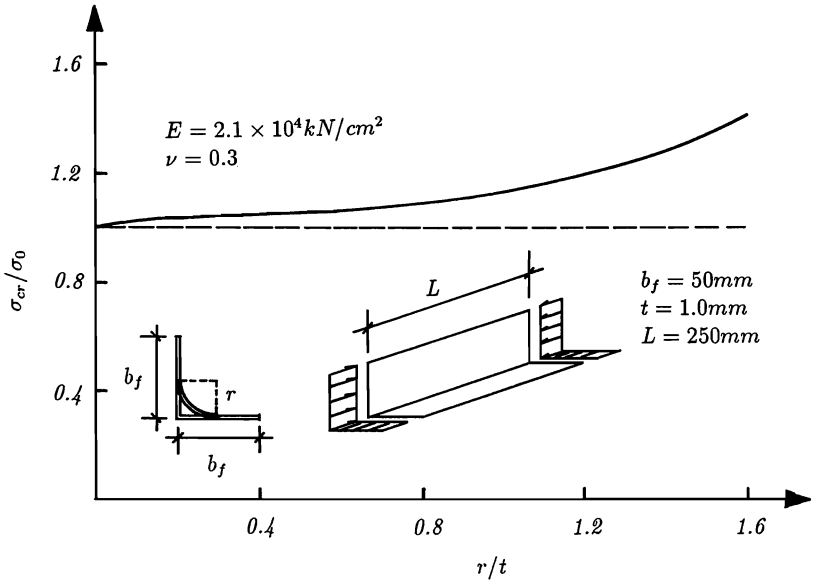

Figure 3: Effect of corner radius on buckling stress

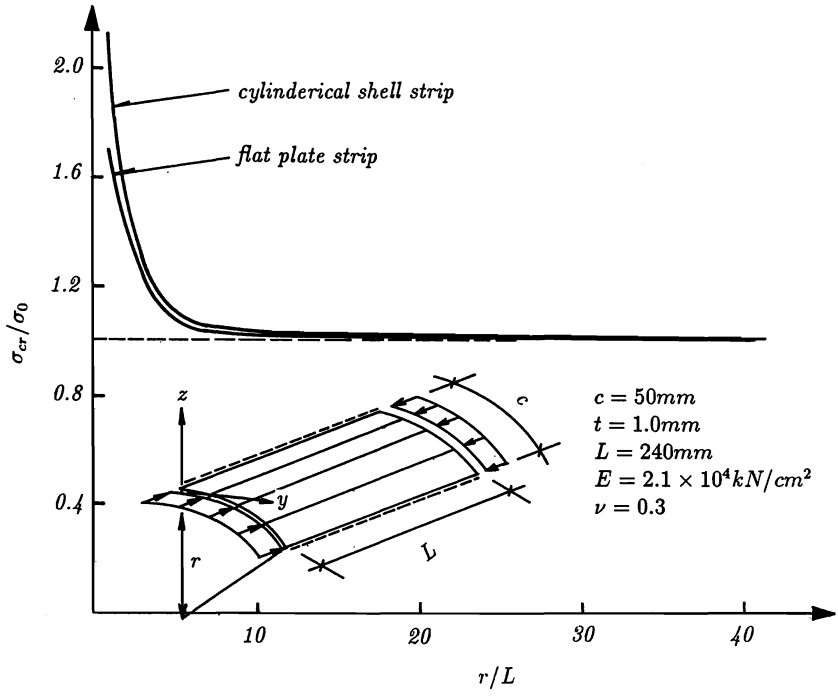

Figure 4: Comparison of flat plate strip results with cylinderical shell strip results

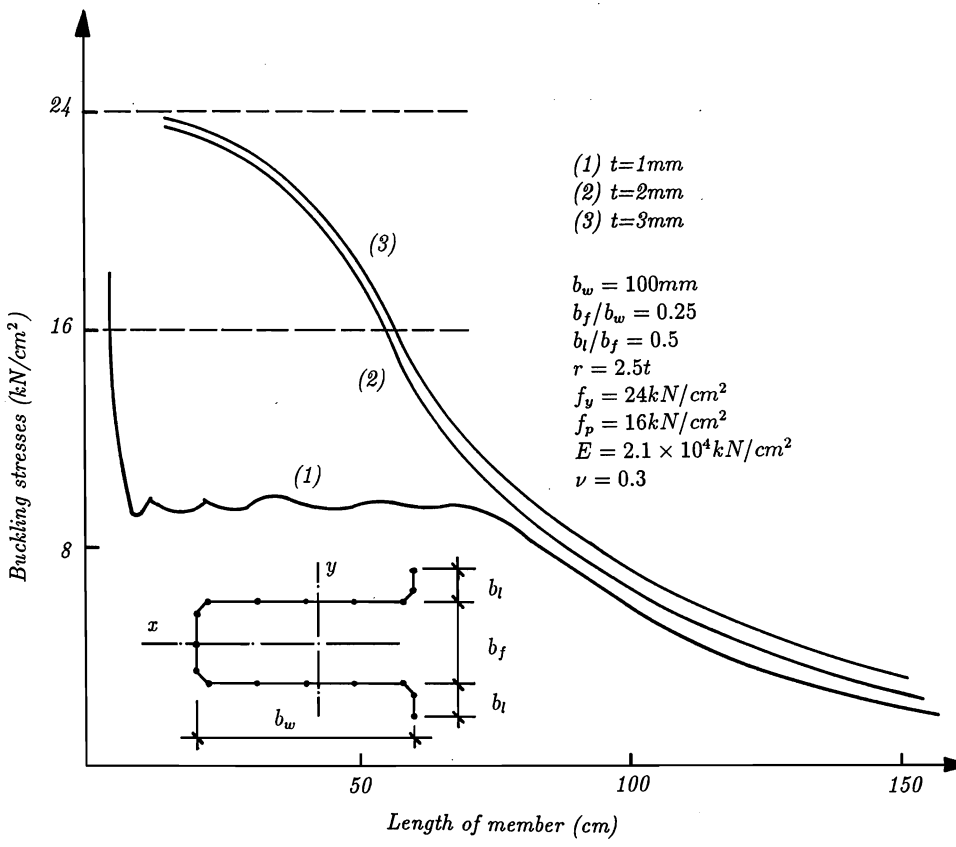

Figure 5: Buckling stress vs length curves of cold-formed columns under uniform compression

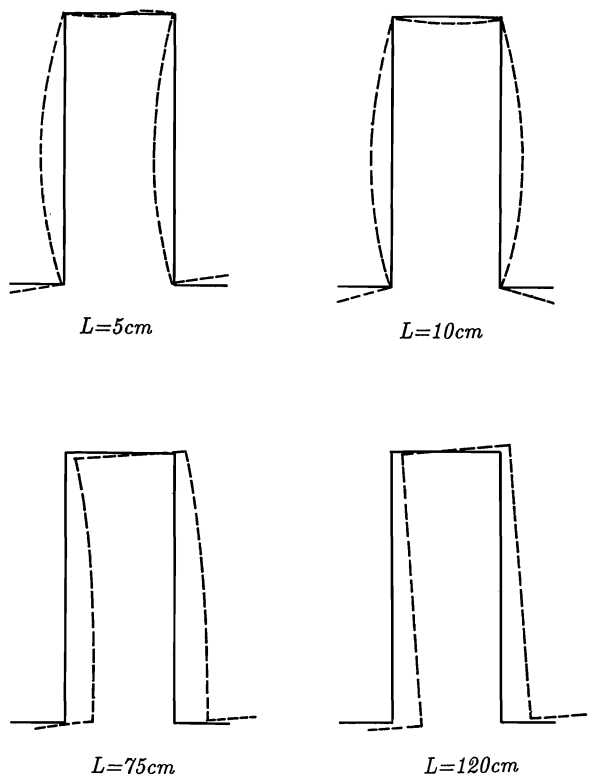

Figure 6: Buckling modes corresponding to curve (1) on the figure 5

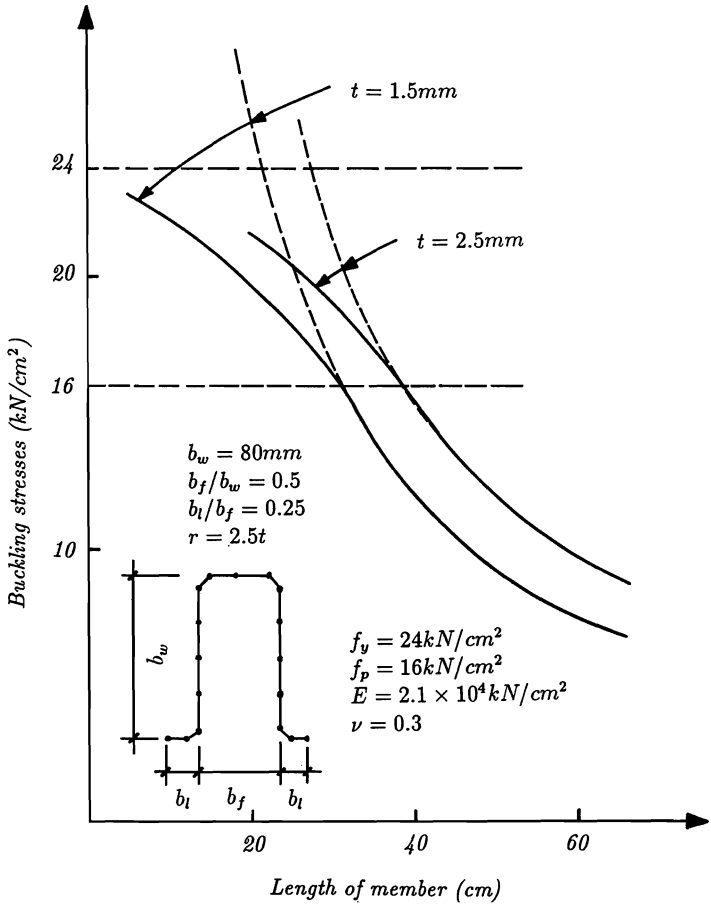

Figure 7: Buckling stress vs length curves of cold-formed columns under uniform compression